PCCP

Accepted Manuscript

ROYAL SOCIETY OF CHEMISTRY

www.rsc.org/pccp

Tuning electronic and magnetic properties of graphenelike AlN nanosheets by surface functionalization and thickness

W. X. Zhang [1], T. Li [1], S. B. Gong [1], C. He[2,*], L. Duan [1]

[1]School of Materials Science and Engineering, Chang'an University, Xi'an 710064, China

[2]State Key Laboratory for Mechanical Behavior of Materials, School of Materials Science and Engineering, Xi'an Jiaotong University, Xi'an 710049, China

Abstract

In this paper, the structural, electronic, and magnetic properties as well as the relative stabilities of fully and partially hydrogenated AlN nanosheets have been systematically investigated by first-principles calculations based on density functional theory. The results indicate that full hydrogenation is more energetically favorable for thinner AlN nanosheets, whereas semi-hydrogenation at N sites is preferred for thicker ones. Moreover, semiconductor → half-metal → metal transition with nonmagnetic → magnetic transfer can be achieved for AlN nanosheets by surface hydrogenation and increasing nanosheet thickness. The diverse electronic and magnetic properties highlight AlN nanosheets potential applications in electronics and spintronics.

* Corresponding Author: C. He; E-mail address: hecheng@mail.xjtu.edu.cn

1. Introduction

Graphene is composed of a single layer of carbon atoms arranged in a two-dimensional (2D) honeycomb lattice. The identification of graphene among mechanically exfoliated graphite nanosheets and the subsequent discovery of its unusual electronic properties[1-3] have led to an extraordinary amount of interest from both academia and industry. The successful isolation of this two-dimensional (2D) crystal wholly refreshed our minds and brought us a new revolution to material science due to its extraordinary structural and electronic properties as well as promising applications in nanoelectronics.[4-8]

The impressive progress in graphene research has motivated scientists to explore other 2D atomic based materials. Among them, AlN nanosheet has become a hotly pursued system as it shares the same honeycomb lattice structure as graphene. AlN nanosheet has aroused extensive research interest due to its many intriguing properties such as high chemical stabilities, excellent mechanical properties and high thermal conductivity.[9-10] The single crystalline AlN nanosheets on Si substrates have been successfully fabricated by a vapor-phase transport method, using Al powder and ammonia as the source materials.[10] Recently, the fascinating electronic properties associated with one-dimensional (1D) fully and partially hydrogenated graphene,[11] BN,[12] ZnO,[13] SiC[14] and AlN[15] nanoribbons derived from either monolayer or multilayer nanosheets heavily depend on the ribbons' width, thickness and edge modification. In contrast, fundamental questions linked to wurtzite AlN sheets remain unexplored. Unlike in its bulk structure, Al and N atoms on the surface of

as-synthesized AlN nanosheets are arranged in planar 3-fold coordination instead of the bulk-like tetrahedral configuration. So the unsaturated sites on Al and N atoms may act as active sites for the adsorption of adatoms to form chemical bonds, and might identify them as promising gas sensors. The interaction of adatoms with polar AlN surfaces has been extensively studied in connection with the unusual instability of polar surfaces. Zhang et al. predicted that AlN nanosheet semi-decorated with hydrogen and fluorine atoms can be a direct or an indirect semiconductor and exhibit completely distinct properties from its pristine forms.[16] Yet a systematically theoretical understanding of electronic and magnetic properties of these functionalized a few AlN layers remains unclear.

Because the interaction of hydrogen with AlN is of great technological interest, compared with the unsaturated bare nanosheets, its band gap change in a hydrogenated AlN nanosheet is an interesting question. In addition, unlike graphene, the surface Al and N atoms in AlN nanosheet have different reacting and bonding natures with H atoms. Therefore, in this paper, the structural, electronic and magnetic properties of fully and partially hydrogenated AlN nanosheets with different thickness are extensive carried out based on first-principles calculations within density functional theory (DFT). These studies provide us a deep understanding of the novel properties of hydrogenated AlN nanosheets, which is essential to employ them as building blocks for future nanodevices.

2. Computational methods

The simulations are based on density functional theory (DFT), which is provided

by DMOL^3.[17-19] The generalized gradient approximation (GGA) with the Perdew-Burke-Ernzerhof scheme (PBE)[20] is adopted for the exchange-correlation potential to optimize geometrical structures and calculate properties for both spin-polarized and spin-unpolarized case.[20] The All-Electron Relativistic Kohn-Sham wave functions and double numeric plus polarization (DNP) basis set are adopted in the local atomic orbital basis set for DMOL^3.[17, 21-22] Pseudopotentials with $3s^2 3p^1$, $2s^2 2p^3$, and H-$1s^1$ valence electron configurations are used for Al, N, and H atoms, respectively. Similar functional have been successfully used to study the structural and electronic properties of H_2O, Si and Cu nanowires.[23-25] The nearest distance between nanosheets in neighboring cells is greater than 15 Å to ensure no interactions between different layers. For geometry optimization, both the cell and the atomic positions are allowed to fully relax. The Brillouin zone is sampled by 6 × 6 × 1 (10 × 10 × 1) *k*-points for all structures in the geometry optimization (electronic) calculations and the real space golbal cutoff radius is set to be 4.8 Å,[26] which brings out the convergence tolerance of energy of 1.0×10^{-5} Ha (1 Ha = 27.2114 eV), maximum force of 0.002 Ha/Å, and maximum displacement of 0.005 Å. Increasing the *k*-points mesh to 8× 8 × 1 for all structures in the geometry optimization does not greatly change the calculated quantities. The electronic distributions of AlN nanosheet are carried out by Mulliken charge analysis, which is performed using a projection of a Linear Combination of Atomic Orbitals (LCAO) basis and to specify quantities such as atomic charge, bond population, charge transfer etc. LCAO supplies better information regarding the localization of the electrons in different atomic layers than a

plane wave basis set does.[24] The obtained relative values of the charge *e*, but not the absolute magnitude, display a high degree of sensitivity to the atomic basis set and a relative distribution of charge.[27]

To evaluate the structural stability of the hydrogenated AlN nanosheets, we calculated the formation energies for both fully and partially hydrogenated systems. The formation energy is defined as the energy difference between the hydrogenated AlN nanosheet, pristine AlN nanosheet, and H_2 molecules.[28] The formation energy (E_f) is expressed as $E_f = E_{AlN\text{-}H} - (\chi_{Al\text{-}N}\mu_{Al\text{-}N} + \chi_H\mu_H)$, where $E_{AlN\text{-}H}$ is the cohesive energy per atom of hydrogenated nanosheet, $\mu_{Al\text{-}N}$ is the cohesive energy per Al-N pair of bulk AlN, μ_H is half of the binding energy of H_2, and $\chi_{Al\text{-}N}$ (χ_H) is the molar fraction of Al-N pairs (H atom) in the hydrogenated systems. According to this definition, a system with smaller E_f value is more favorable.

3. Results and discussion

The AlN nanosheets were constructed from the bulk phase, with the thickness ranging from one to five bilayers (a bilayer is composed of two closely adjacent layers, one for Al and the other for N, e.g., the AlN nanosheet in Fig. 1a contains two bilayers). We began our study with AlN hexagonal wurtzite (WZ) structure with P63mc space group. The Al-N bond lengths within one bilayer and those between two adjacent bilayers are calculated to be 1.883 and 1.927 Å, respectively. The accuracy of our calculation procedure is also tested using pristine monolayer AlN nanosheet. A 4 × 4 × 1 supercell of monolayer AlN nanosheet containing 32 atoms is constructed. Each N atom has three covalent bonds with the three adjacent Al atoms and two

residual electrons per every N atom form a lone pair distributed perpendicularly to the sheet's plane such that all orbitals in AlN nanosheet exhibit a sp^2-hybridization. The optimized lattice constant of 3.112 Å and bond length of Al-N of 1.797 Å are in good agreement with theoretical value of 3.121 Å and 1.808 Å, respectively.[29,30] The calculated indirect band gap of AlN sheet (Fig. 1) is also in good agreement with previous theoretical results.[30-32]

Next we studied 2D nanosheets derived from bulk AlN with different layers. AlN nanosheets composed of one to five bilayers transform from the initial wurtzite configuration to a flat graphitic structure after geometry optimization, and a two-bilayer-thick AlN nanosheet is shown in Fig. 1. In this case, the geometry change is obvious: the atoms within each bilayer converge to just one planar layer, accompanied by a little Al-N bond expansion (1.797~1.808 Å) within each bilayer and the interlayer distance expansion (2.183~2.261 Å). Moreover, the bond angle within the newly formed planar layer increases from the wurtzite tetrahedral, 112° on average, to plane trigonal, ~120°. Similar to the single-layer hexagonal AlN, the two-layer graphitic AlN is also a semiconductor with a indirect band gap of 4.16 eV (Fig. 1b), which is larger than other theoretical value of 2.93eV by GGA-PAW potential implemented in the Vienna *ab initio* simulation package.[33] All the graphitic AlN nanosheets considered here are semiconductors, and the band gap as a function of bilayer thickness are 4.27, 4.16, 4.02, 3.89, and 3.73 eV for one, three, four, and five bilayers, respectively. It seems that the band gap monotonically decreases with increasing bilayer number. The larger band gaps for the thinner nanosheets are an

indication of quantum size effect.[6, 8]

In order to take into account the contributions of the van der Waals (vdW) interactions between different layers, the DFT-D (D stands for dispersion) approach within the Grimme scheme is adopted for the vdW correction.[34] This method has been successfully applied in previous studies of the interaction between silicene on MoS_2 and benzene on Cu (100) surfaces.[35]

Similar to DFT results, two-bilayer-thick AlN nanosheet transform from the initial wurtzite configuration to a flat graphitic structure after geometry optimization. The Al-N bond within each bilayer, the interlayer distance and the bond angle within the newly formed planar layer are 1.800 Å, 2.214 Å, and 119.641°, respectively, obtained by DFT-D approach. The two-layer graphitic AlN is also a semiconductor with a indirect band gap of 4.21 eV. With increasing bilayer number of AlN nanosheets, the electronic and magnetic properties obtained by DFT-D method exhibit the same trends with DFT results and vdW interlayer interactions hardly influence the electronic states near Femi level.[36] Our test computations have shown that for unstatured AlN nanosheets, the electronic and magnetic properties have no noticeable differences between DFT and DFT-D methods, which is consistent with previous results.[37,38] In addition, although the hybrid functionals HSE,[39] PBE0,[40] or B3LYP,[41,42] represent the state-of-the-art approach to accurately evaluate the band structures, the hybrid functionals are very time consuming and would quickly become prohibitively expensive as increasing of the system size. In this work, it is required only to predict the reasonable trends for changes of electronic and magnetic properties. Thus, it is

considered that GGA-DFT based calculations should be enough as long as all the calculations use the same settings.[43]

Following the idea of hydrogenated graphane,[11] GaN,[25] ZnO,[28] and *h*-BN[44] nanosheets, we then studied fully hydrogenated AlN nanosheets with different thicknesses (labeled as *n*-H-AlN-H, where n refers to the number of bilayers). Fig. 2 presents the atomic structure, band structure, and density of states (DOS) of fully hydrogenated one-bilayer (1-H-AlN-H, Fig. 2a) and two-bilayer (2-H-AlN-H, Fig. 2b) nanosheets, respectively. The Al and N atoms become sp^3 hybridized with H atoms bonded, which distorts the planar geometry forming a zigzag configuration. The optimized Al-H bond lengths (1.581 and 1.584 Å, respectively, for the hydrogenated one-bilayer and two-bilayer nanosheets) and N-H bond lengths (1.029 Å) indicate the formation of strong chemical bonds between hydrogen and surface atoms. The bond angles $\angle_{\text{HNAl-1}}$ ($\angle_{\text{HNAl-2}}$), $\angle_{\text{HAlN-1}}$ ($\angle_{\text{HAlN-2}}$), $\angle$AlNAl-1 ($\angle_{\text{AlNAl-2}}$), and $\angle_{\text{NAlN-1}}$ ($\angle_{\text{NAlN-2}}$) corresponding to 1-H-AlN-H (2-H-AlN-H) are 111.3° (111.1°), 111.3° (112.8°), 107.6°(105.9), and 107.6°(106.2) on average, respectively. The optimized structural parameters suggest that the fully hydrogenated nanosheet retains the initial wurtzite configuration rather than the graphitic one. The atomic charge transfers in AlN nanosheets are analyzed by the Mulliken charge analysis.[23,24,26] The results indicate that H atoms adsorbed on Al and N atoms are carrying charges of -0.030 (-0.070) and 0.181 (0.175) electrons for 1-H-AlN-H (2-H-AlN-H), respectively.

Similar to graphene or monolayer BN nanosheets, the fully hydrogenated one-bilayer nanosheet (1-H-AlN-H) is a nonmagnetic semiconductor, with an indirect

band gap of 3.86 eV, smaller than that of a bare AlN graphitic nanosheet (4.27 eV). The band gap of the hydrogenated nanosheet is decreased with the thickness of AlN nanosheets. The fully hydrogenated two-bilayer nanosheet (2-H-AlN-H) is also a nonmagnetic semiconductor, with an indirect band gap of 2.28 eV. The comparison results between DFT and DFT-D methods for 1-H-AlN-H, and 2-H-AlN-H systems are summerized in Table 1, which are very similar. Therefore, in the following work, in order to speed up the calculation, the DFT method is employed. The results of BS exhibit different trends with Zhang's theoretical study by GGA-PAW potential.[33] Moreover, the hydrogenated nanosheets with thicknesses greater than four bilayer are all metallic. As exemplified in Fig. 2c, the hydrogenated four-bilayer nanosheet (4-H-AlN-H) becomes a nonmagnetic metal.

Here we see some differences between fully hydrogenated graphene and AlN nanosheet. Hydrogenation opens a band gap in the former while it reduces the band gap in the latter. In fact, introduction of two H atoms introduces occupied energy bands in PDOS of Fig. 2c. These are located just above the valence band of pristine AlN nanosheet. Accordingly, the band gap of the system is reduced. With the thickness increasing in AlN nanostructures, electrons occupy the 2*p* states of surface N atoms and 3*p* states of surface Al atoms. The hybridized bonding state is located at the valence band maximum (VBM) and partially occupied, leading to the metallic behavior, which is consolidated by the projected DOS (PDOS) in Fig. 2c. Bare AlN nanosheets favor flat graphitic structures after relaxation and are semiconductors. In contrast, all fully hydrogenated AlN nanosheets adopt the wurtzite configurations.

This obvious difference indicates that the structural and electronic properties of AlN nanosheets are very sensitive to surface decoration.

Similar to Zn and O sites in ZnO nanosheets, Al and N sites in AlN nanosheets are chemically nonequivalent, and then semi-hydrogenation can be achieved by merely saturating either all the Al sites or all the N sites. We first studied semi-hydrogenation on Al sites for AlN nanosheets with different numbers of bilayers (denoted as *n*-H-AlN).

In Fig. 3, we summarize the results of semi-hydrogenated AlN nanosheets with one, two and three bilayers. In all cases, spin polarization is evident in the band structure and PDOS. In fact, semi-hydrogenation on Al atoms forms strong Al-H bonds and leaves the dangling bonds of surface Al atoms spin unpaired. The origin of the magnetic behavior are further investigated by plotting the spin density distribution (Fig. 3). Obviously, the emergent spin polarization is not restricted to the surface N atoms but instead is delocalized uniformly in the entire system, leading to a net magnetic moment of approximately 0.66, 0.38, 0.27, and 0.16 μ_B per unit cell for one, two, three, and four bilayers, respectively. The magnetic moment monotonically decreases as the thickness's increase, while in the theoretical study by GGA-PAW potential, the net magnetic moment for different layers of H-AlN systems keeps a constant as 1 μ_B.[33]

In pristine AlN nanosheet, the charge transfer from Al to N and the orbital hybridization make electrons paired and the system is nonmagnetic. When semihydrogenated on Al sites, Al atoms are covalently bonded with H atoms forming

sp^3 hybridization and almost no charge transfer occurs from Al to N. 2*p* electrons on N atoms remain unpaired. Thus, The induced magnetism is attributed primarily to unsaturated N atoms (2*p* orbital) and H atoms (1*s* orbital), which is corresponding to the results as found in ZnO[28] and graphone[11] nanosheets.

More careful examination of the band structure of *n*-H-AlN reveals appealing properties associated with this novel system. As described in Fig. 3a, the hydrogenated one bilayer system (1-H-AlN) behaves as a magnetic semiconductor with indirect band gaps of 5.54 and 0.41 eV in the spin-up and spin-down states, respectively. The absorption of H atom on Al sites introduces a low acceptor level located slightly above the VBM only in the spin-down state, resulting in hole-doping *p*-type semiconductivity. However, when the thickness increases to two bilayers, the resulting 2-H-AlN becomes a magnetic half-metal. As clearly seen in Fig. 3b, the spin-up state behaves as a semiconductor with an indirect band gap of 5.21 eV, whereas the spin-down state turns metallic. When the number of bilayers further increases to three, both the spin-up and spin-down states become metallic, as can be seen in c in Fig. 3. The situation for four bilayers is similar to that of three, indicating that the semi-hydrogenated multilayer nanosheets are all metals with strong spin polarization. In the theoretical study by GGA-PAW potential, for odd number of bilayers in *n*-H-AlN, the systems are magnetic semiconductors, while for even number of bilayers, half-metallic character are observed.[33]

By increasing the thickness, both occupied spin-up and unoccupied spin-down channels are broadened because of the hybridization effect, which makes the Fermi

level lie in the H-induced bands and gives rise to half-metallic or metallic behaviors. Thus, with semi-hydrogenation restricted on the surface Al atoms, a magnetic *p*-type semiconductor → half-metal → metal transition can be tuned by varying the nanosheet thickness.

Fig. 4 presents the results of semi-hydrogenation on N sites (denoted as *n*-AlN-H), in one-bilayer and four-bilayer. In contrast with *n*-H-AlN, *n*-AlN-H is practically a nonmagnetic metal. Moreover, all semi-hydrogenated systems on N sites are strikingly metallic irrespective of thickness. As mentioned above, the induced metallicity is attributed to the partially occupied surface state, which is not completely removed after hydrogen passivation.

Finally, we summarize the computed properties for hydrogenated AlN nanosheets in Fig. 5. Clearly, the intriguing and diverse transformation in electronic and magnetic properties of the novel AlN systems remarkably depends on hydrogenation sites and nanosheet thickness. Our results predict that effectively controlling the hydrogenation sites and nanosheet thickness is a tunable way to modulate the properties of AlN nanosheets, and that a semiconductor → half-metal → metal (nonmagnetic-magnetic) transition can be achieved. These diverse properties are of fundamental significance and open up exciting opportunities for the design of novel nanoelectronic spintronic devices.

Fig. 6 shows the relative stability of different AlN systems as a function of bilayer number. For the semi-hydrogenated case (*n*-AlN-H or *n*-H-AlN), the comparison of relative stability is straightforward: the formation energy progressively

decreases with increasing bilayer number, which suggests that thicker nanosheets are more likely to be accessible; moreover, for all the AlN nanosheets considered, semi-hydrogenated ones at Al sites are the least stable. However, the fully hydrogenated systems are more complicated. When the thickness is fewer than three bilayers, the fully hydrogenated system (*n*-H-AlN-H) is more favorable than its semi-hydrogenated counterpart, but for thicker nanosheets the most stable system is *n*-AlN-H.

The relative stability of different AlN systems could also be proved by the changes of bond length and charge transfer. The results indicate that H atoms adsorbed on N atoms are carrying charges of 0.181 (0.157) and 0.175 (0.153) electrons for 1-H-AlN-H (1-AlN-H) and 2-H-AlN-H (2-AlN-H), respectively. Therefore, the charge transfers in 1-H-AlN-H and 2-H-AlN-H are more chemically active than 1-AlN-H and 2-AlN-H, because it has more electrons. Meanwhile, the N-H bond lengths in 1-H-AlN-H and 2-H-AlN-H are the same as 1.029 Å, which are shorter than these in 1-AlN-H (1.041 Å) and 2-AlN-H (1.032 Å), respectively. The N-H bond lengths decide the energy of covalent bond,[6] which are corresponding to the results of formation energies of Fig. 6. Meanwhile, the comparison results between DFT and DFT-D methods for 1-H-AlN-H, 2-H-AlN-H, 1-AlN-H and 2-AlN-H systems have shown in Table 1.

4. Conclusions

In summary, we have systematically investigated the modulation of structural, electronic and magnetic properties through hydrogenation of AlN nanosheets using

first-principles calculations. The main conclusions are as follows. (1) Bare wurtzite AlN nanosheets within five bilayers adopt graphite-like structures after atomic relaxation. (2) The fully hydrogenated AlN nanosheets within three bilayers are indirect band gap semiconductors, whereas those with thicker bilayers become metallic. (3) The semi-hydrogenated nanosheets on Al sites are all magnetic, and a semiconductor → half-metal → metal transition occurs with increasing nanosheet thickness. (4) Semi-hydrogenation on N sites results in nonmagnetic metallicity in AlN nanosheets. Therefore, surface passivation by hydrogen serves as an important approach in tailoring the electronic and magnetic properties of low-dimensional AlN nanosheets. The diverse properties of hydrogenated AlN nanosheets have the potential for wider applications of 2D-based materials and devices.

Acknowledgements

The authors acknowledge supports by National Natural Science Foundation of China (NSFC, Nos. 51177006, 51102023, 51301020 and 51471124), Natural Science Foundation of Shaanxi province, China (2014JQ6196, 2014JQ6217, 2014JQ6212 and 2013JM8017), Ph.D. Programs Foundation of Ministry of Education of China (Grant No. 20110201120002), the special fund for basic scientific research of central colleges of Chang'an University (No. 2013G1311053) and State Key Laboratory for Mechanical Behavior of Materials.

References

1. K. S. Novoselov, A. K. Geim, S. V. Morozov, D. Jiang, M. I. Katsnelson, I. V. Grigorieva, S. V. Dubonos, and A. A. Firsov, *Nature* 2005, **438**, 197.
2. R. R. Nair, I. L. Tsai, M. Sepioni, O. Lehtinen, J. Keinonen, A. V. Krasheninnikov, A. H. Castro Neto, M. I. Katsnelson, A. K. Geim, and I. V. Grigorieva, Nat. Commun., 2013, 4, 2010.
3. A. K. Geim, and K. S. Novoselov, *Nat. Mater.* 2007, **6**, 183.
4. Y. B. Zhang, Y. W. Tan, H. L. Stormer, and P. Kim, *Nature* 2005, **438**, 201.
5. S. V. Morozov, K. S. Novoselov, M. I. Katsnelson, F. Schedin, D. C. Elias, J. A. Jaszczak, and A. K. Geim, *Phys. Rev. Lett.* 2008, **100**, 016602.
6. C. Q. Sun, Nanoscale, 2010, 2, 1930.
7. K. S. Novoselov, Z. Jiang, Y. Zhang, S. V. Morozov, H. L. Stormer, U. Zeitler, J. C. Maan, G. S. Boebinger, P. Kim, and A. K. Geim, *Science* 2007, **315**, 1379.
8. C. C. Yang, and S. Li, J. Phys. Chem. B, 2009, 113, 14207.
9. Y. Taniyasu, and M. Kasu, *Appl. Phys. Lett.* 2011, **98**, 131910.
10. P. Tsipas, S. Kassavetis, D. Tsoutsou, E. Xenogiannopoulou, E. Golias, S. A. Giamini, C. Grazianetti, D. Chiappe, A. Molle, M. Fanciulli, and A. Dimoulas, *Appl. Phys. Lett.* 2013, **103**, 251605.
11. J. Zhou, Q. Wang, Q. Sun, X. S. Chen, Y. Kawazoe, and P. Jena, *Nano Lett.* 2009, **9**, 3867.
12. W. Chen, Y. Li, G. Yu, C. Li, S. B. Zhang, Z. Zhou, and Z. Chen, *J. Am. Chem. Soc.* 2010, **132**, 1699.
13. L. Kou, C. Li, Z. Zhang, and W. Guo, *ACS Nano* 2010, **4**, 2124.

14. X. B. Li, C. W. Mi, F. C. Meng, and I. H. Lee, *Comp. Mater. Sci.* 2013, **78**, 129.

15. A. J. Du, Z. H. Zhu, Y. Chen, G. Q. Lu, and S. C. Smith, *Chem. Phys. Lett.* 2009, **469** 183.

16. C. W. Zhang, and P. J. Wang, *Phys. Lett. A* 2011, **375**, 3583.

17. H. Y. He, J. Hu, and B. C. Pan, *J. Chem. Phys.* 2009, **130**, 204516.

18. G. A. Gelves, B. Lin, U. Sundararaj, and J. A. Haber, *Adv. Funct. Mater.* 2006, **16**, 2423.

19. B. Delley, *J. Chem. Phys.* 1990, **92**, 508.

20. J. P. Perdew, K. Burke, and M. Ernzerhof, *Phys. Rev. Lett.* 1996, **77**, 3865.

21. Y. F. Zhu, Q. Q. Dai, M. Zhao, and Q. Jiang, Sci. Rep. 2013, 3, 1524.

22. Z. M. Ao, and F. M. Peeters, Appl. Phys. Lett., 2010, 96, 253106.

23. R. Q. Zhang, W. T. Zheng, and Q. Jiang, *J. Phys. Chem. C*, 2009, **113**, 10384.

24. C. He, P. Zhang, Y. F. Zhu, and Q. Jiang, *J. Phys. Chem. C* 2008, **112**, 9045.

25. M. X. Xiao, T. Z. Yao, Z. M. Ao, P. Wei, D. H. Wang, and H. Y. Song, *Phys. Chem. Chem. Phys.* 2015, DOI: 10.1039/C4CP05788K.

26. M. D. Segall, P. L.D. Lindan, M. J. Probert, C. J. Pickard, P. J. Hasnip, S. J. Clark, and M. C. Payne, *J. Phys. Condens. Matter.* 2002, **14**, 2717.

27. E. R. Davidson, and S. Chakravorty, *Theor. Chim. Acta* 1992, **83**, 319.

28. Q. Tang, Y. F. Li, Z. Zhou, Y. S. Chen, and Z. F. Chen, *Appl. Mat. Interfaces* 2010, **2**, 2442.

29. S. Valedbagi, A. Fathalian, and S. MohammadElahi, *Optics Commun.* 2013, **309**, 153.

30. Y. Jiao, A. Du, Z. Zhu, V. Rudolph, S.C. Smith, *J. Phys. Chem. C* 2010, **114**, 7846.

31. H. W. Cao, P. F. Lu, Z. Y. Yu, J. Chen, and S. M. Wang, *Superlattices Microstruct.* 2014, **73**, 113.

32. S. F. Rastegara, A. A. Peyghana, H. R. Ghenaatianb, and N. L. Hadipour, *Appl. Surf. Sci.* 2013, **274**, 217.

33. C. W. Zhang, and F. B. Zheng, *J. Comput. Chem.* 2011, **32**, 3122.

34. S. Grimme, *J. Comput. Chem.* 2006, **27**, 1787.

35. M. Robledo, G. Pacchioni, F. Martín, M. Alcamí, and S. Díaz-Tendero, *J. Phys. Chem. C* 2015, **119**, 4062.

36. X. F. Chen, Y. F. Zhu, and Q. Jiang, *RSC Adv.* 2014, **4**, 4146.

37. T. P. Kaloni, Y. C. Cheng, and U. Schwingenschlogl, *J. Appl. Phys.* 2013, **113**, 104305.

38. N. Gao, J. C. Li, and Q. Jiang, *Phys. Chem. Chem. Phys.* 2014, **16**, 11673.

39. J. Heyd, and G. E. Scuseria, *J. Chem. Phys.* 2004, **121**, 1187.

40. J. Heyd, G. E. Scuseria, and M. Ernzerhof, *J. Chem. Phys.* 2003, **118**, 8207.

41. P. J. Stephens, F. J. Devlin, C. F. Chabalowski, and M. J. Frisch, *J. Phys. Chem.* 1994, **98**, 11623.

42. A. D. Becke, *J. Chem. Phys.* 1993, **98**, 5648.

43. L. Dong, S. K. Yadav, R. Ramprasad, and S. P. Alpay, *Appl. Phys. Lett.* 2010, **96**, 202106.

44. J. Zhou, Q. Wang, Q. Sun, and P. Jena, *Phys. Rev. B* 2010, **81**, 085442.

Table 1 The comparison results between DFT and DFT-D methods for 1-H-AlN-H, 2-H-AlN-H, 1-AlN-H and 2-AlN-H systems.

		Bond type	Bond length (Å)	Charge (e)	E_g (eV)
DFT	1-H-AlN-H	Al-H	1.581	H on Al -0.030	3.86
		N-H	1.029	H on N 0.181	
	2-H-AlN-H	Al-H	1.584	H on Al -0.070	2.28
		N-H	1.029	H on N 0.175	
	1-AlN-H	N-H	1.041	H on N 0.157	Metallic
	2-AlN-H	N-H	1.032	H on N 0.153	Metallic
DFT-D	1-H-AlN-H	Al-H	1.577	H on Al -0.032	3.89
		N-H	1.030	H on N 0.181	
	2-H-AlN-H	Al-H	1.579	H on Al -0.074	2.31
		N-H	1.030	H on N 0.175	
	1-AlN-H	N-H	1.042	H on N 0.152	Metallic
	2-AlN-H	N-H	1.033	H on N 0.159	Metallic

Captions

Fig. 1. Structure of AlN nanosheets with two bilayers: (a) initial wurtzite structure and (b) optimized structure. The purple and blue balls represent Al and N atoms, respectively, and the numbers are bond length or interlayer distance in Å. (c) Band structure of graphene-like AlN. Fermi level is set to zero.

Fig. 2. Optimized geometry and band structure for fully hydrogenated (a) one-bilayer (1-H- AlN-H), (b) two-bilayer (2-H- AlN-H) nanosheets and (c) four-bilayer (4-H-AlN-H) nanosheets. Purple, blue and white balls represent Al, N, and H atoms, respectively. PDOS results are also shown for selected atomic orbitals in b and c.Q

Fig. 3. Optimized geometric structure (side view), band structure, PDOS, and spin density distribution of (a) 1-H-AlN, (b) 2-H-AlN, and (c) 3-H-AlN, respectively. (d) Zoom of the region near the Fermi level for the spin-up band structure of c. The isosurface is set to be 0.05 e/Å^3.

Fig. 4. Optimized geometry (side view) and band structure for (a) 1-AlN-H and (b) 2-AlN-H with PDOS.

Fig. 5. Summary of the electronic and magnetic properties of (a) *n*-H-AlN-H, (b) *n*-H- AlN, and (c) *n*-AlN-H with different numbers of bilayers.

Fig. 6. Formation energies of hydrogenated AlN nanosheets as a function of bilayer number, *n*. ■, ●, and ▲denote H-AlN, AlN-H and H-AlN-H, respectively.

Fig. 1

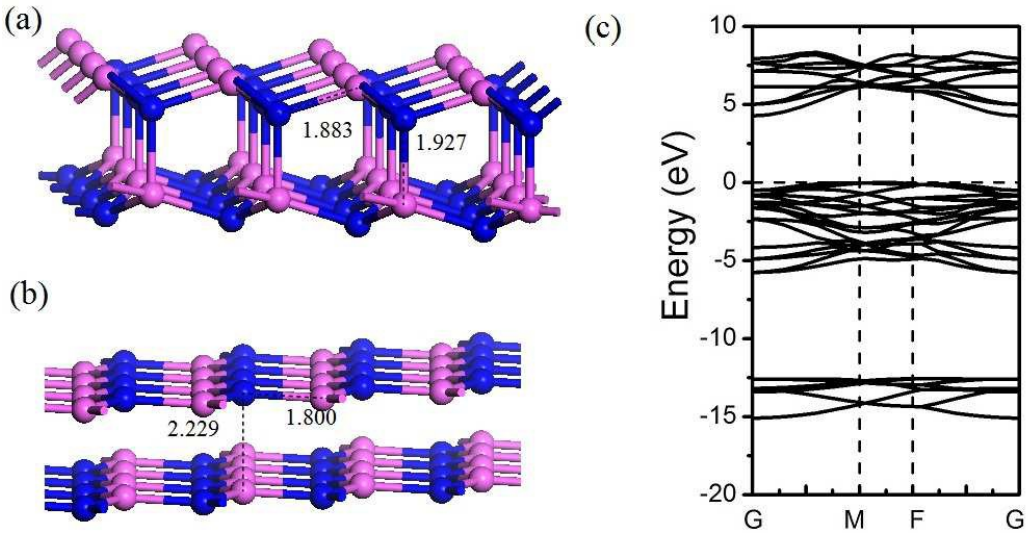

Fig. 2

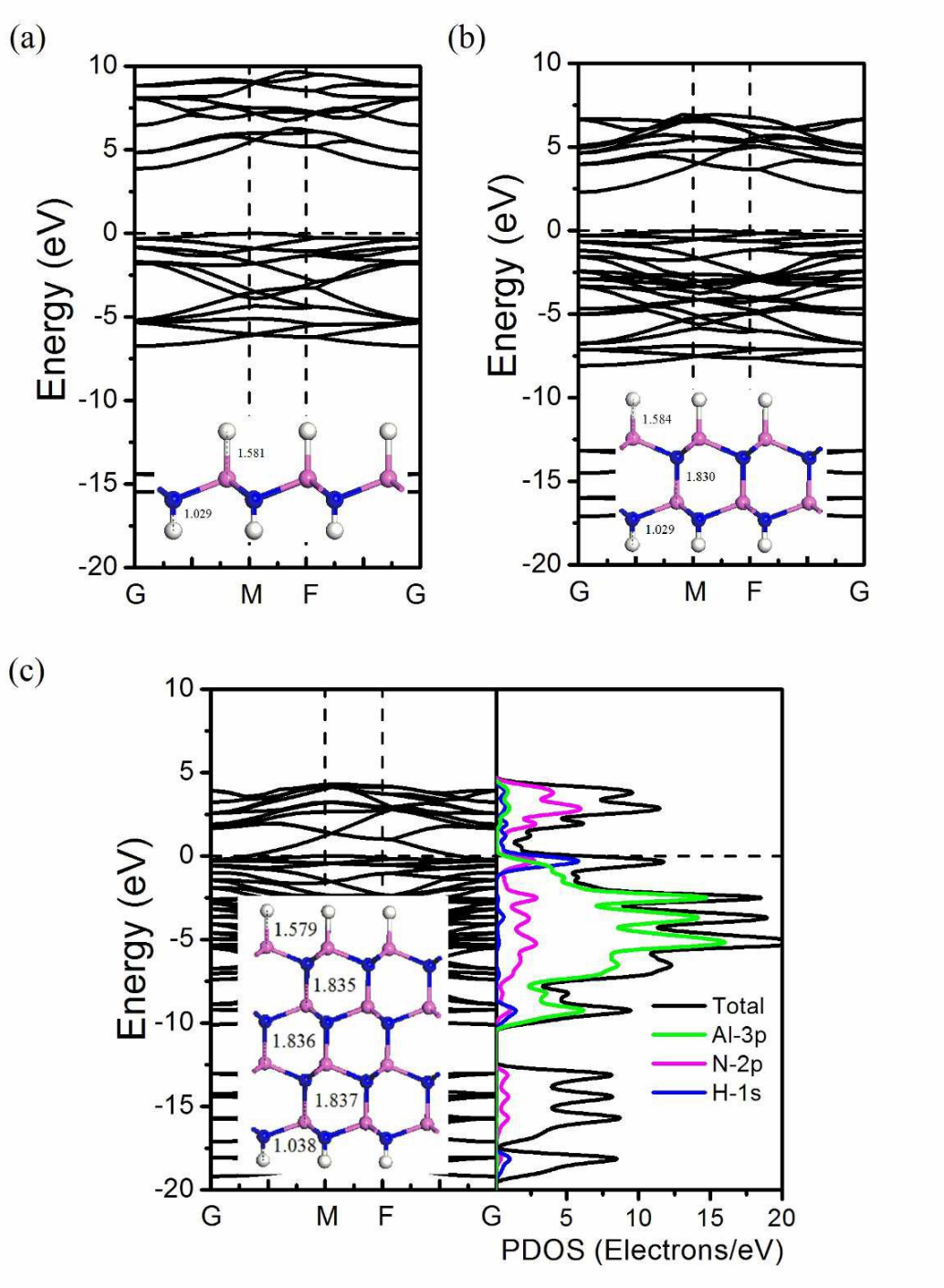

Fig. 3

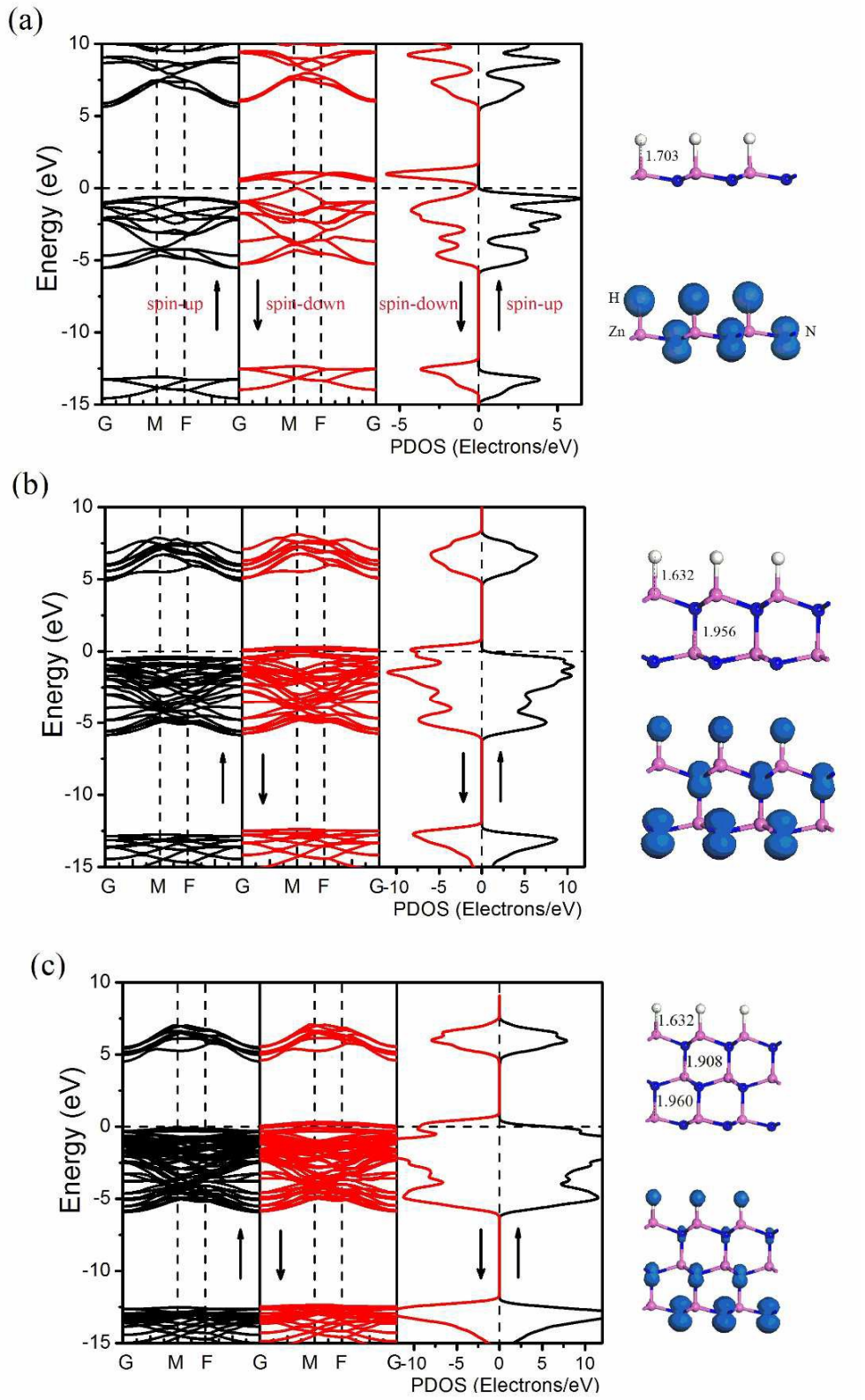

Fig. 4

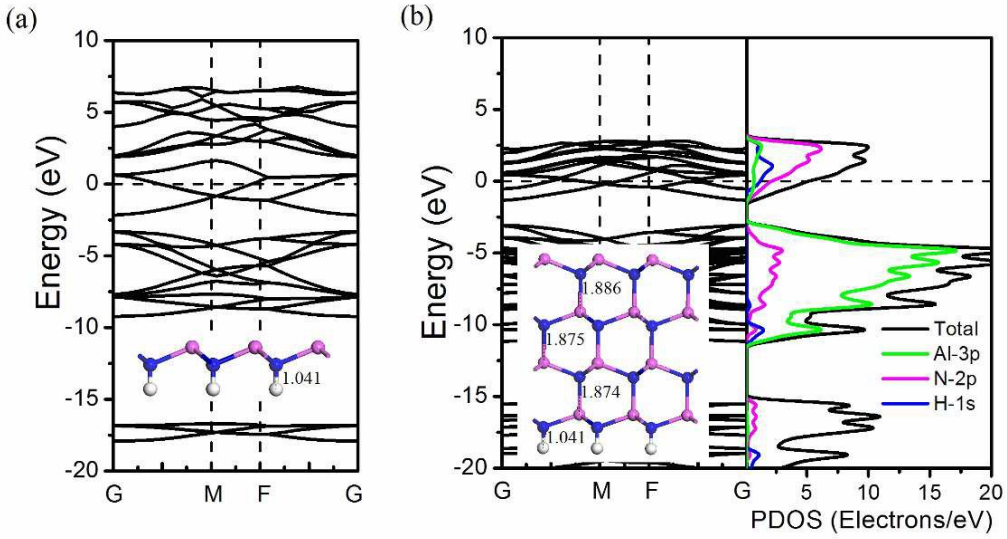

Fig. 5

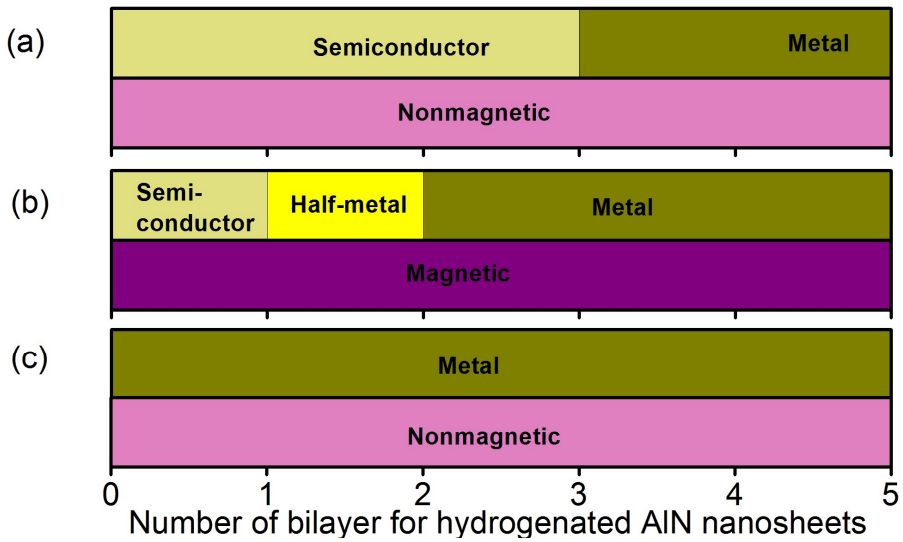

Fig. 6